Syntheses, crystal structures and properties of silver(I) and copper(II) complexes with an oxazoline-containing tetradentate ligand†‡

Yong-Qing Huang,[ab] Guang-Xiang Liu,[a] Xia-Ying Zhou,[a] Taka-aki Okamura,[c] Zhi Su,[a] Jian Fan,[a] Wei-Yin Sun,*[a] Jin-Quan Yu*[d] and Norikazu Ueyama[c]

Received (in Montpellier, France) 4th February 2010, Accepted 12th April 2010
DOI: 10.1039/c0nj00092b

Six new coordination complexes, $[AgL]CF_3SO_3$ (**1** and **2**), $[Ag_2L_2](NO_3)_2{\cdot}4CH_3NO_2$ (**3**), $[AgL]NO_3{\cdot}0.5CH_3OH$ (**4**), $[AgL]BF_4$ (**5**) and $[Cu_4L_2(OCH_3)_2(OH)_2(NO_3)_2](NO_3)_2{\cdot}0.32H_2O$ (**6**), were obtained by reactions of the corresponding metal salts with ligand *N*,*N*′-bis[4-(4,5-dihydrooxazol-2-yl)-benzyl]ethane-1,2-diamine (L). The results of X-ray crystallographic analysis indicate that complexes **1** and **2** are supramolecular isomers with a wavelike cationic two-dimensional network structure of **1** and a double-stranded helical chain of **2**. Complexes **4** and **5** also have helical chain structures with *P* and *M* forms. Differing from polymeric structure of **1**, **2**, **4** and **5**, complexes **3** and **6** are a M_2L_2 molecular rectangle and a M_4L_2 cage, respectively. The results show that the flexible ligand L can have different conformation and coordination modes leading to complexes with varying structures. Magnetic data show that there are antiferromagnetic interactions in the dimeric unit of complex **6**.

Introduction

In recent years, a great deal of effort has been devoted to the assembly of metal–organic frameworks (MOFs) with multidentate organic ligands, due to their novel structures and topologies, as well as their interesting properties and potential applications in optics, magnetism and catalysis, *etc*.[1–4] In contrast to the rigid ligands that show little or no conformational changes when they interact with metal salts, flexible multidentate ligands can adopt different conformations and have more possible coordination modes according to the different geometric requirements of metal ions. Currently, many interesting structures with flexible multidentate ligands such as rotaxanes, catenanes, helicates and infinite one-dimensional (1D) chains, two-dimensional (2D) networks and three-dimensional (3D) frameworks have been reported.[5] However, it is still a great challenge for chemists to design and synthesize MOFs with predicted structures and topologies when the ligands with more than two coordination sites are flexible.

In our previous work, we have systematically studied the assembly reactions of a series of di-Schiff base and reduced di-Schiff base ligands with flexible $-CH_2CH_2-$ spacers, such as 1,2-bis(4-pyridylmethylamino)ethane (L1), 1,2-bis(4-pyridylmethyleneimino)ethane (L2), 1,2-bis(3-pyridylmethylamino)-ethane (L3) and 1,2-bis(3-pyridylmethyleneimino)ethane (L4) with various metal salts and obtained MOFs with different structures and properties.[6] For example, complexes $[Ag_2(L2)_2](CF_3SO_3)_2$ with an infinite chain-like structure and $[Ag_3(L2)_2](NO_3)_3{\cdot}H_2O$ with an infinite 2D network were obtained by assembly of L2 with $AgCF_3SO_3$ and $AgNO_3$, respectively, in which L2 is tridentate in the former and tetradentate in the latter.[6c] The results demonstrate that such multidentate ligands are versatile and can adopt different conformations when they interact with metal salts as a consequence of their flexibility. For further studies on assembly of flexible multidentate ligand with transition metal salts, we designed and synthesized a new reduced di-Schiff base multidentate ligand *N*,*N*′-bis(4-(2-oxazolinyl)benzyl)ethane-1,2-diamine (L) (Scheme 1). The flexible multidentate ligands with pyridyl groups are well studied,[6] while those with oxazolinyl groups have not up to now been documented. In this paper, six new coordination complexes, $[AgL]CF_3SO_3$ (**1** and **2**), $[Ag_2L_2](NO_3)_2{\cdot}4CH_3NO_2$ (**3**), $[AgL]NO_3{\cdot}0.5CH_3OH$ (**4**), $[AgL]BF_4$ (**5**) and $[Cu_4L_2(OCH_3)_2(OH)_2(NO_3)_2](NO_3)_2{\cdot}0.32H_2O$ (**6**), were obtained by assembly of L with different Ag(I) and Cu(II) salts, respectively. Herein, we report the synthesis, crystal structures and properties of these complexes.

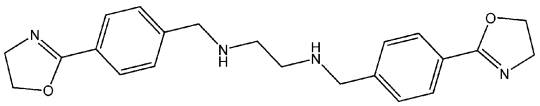

Scheme 1 Structure of the ligand L.

[a] *Coordination Chemistry Institute, State Key Laboratory of Coordination Chemistry, School of Chemistry and Chemical Engineering, Nanjing National Laboratory of Microstructures, Nanjing University, Nanjing 210093 China. E-mail: sunwy@nju.edu.cn; Fax: +86 25 8331 4502*
[b] *Department of Applied Chemistry, College of Chemical and Environmental Engineering, Shandong University of Science and Technology, Qingdao 266510, China*
[c] *Department of Macromolecular Science, Graduate School of Science, Osaka University, Toyonaka, Osaka 560-0043, Japan*
[d] *Department of Chemistry, The Scripps Research Institute, La Jolla, CA 92037, USA*

† CCDC reference numbers for compounds **1–6**: 765656–765661. For crystallographic data in CIF or other electronic format see DOI: 10.1039/c0nj00092b

‡ This article is part of a themed issue on Coordination polymers: structure and function.

Experimental section

Materials and measurements

All commercially available chemicals are of reagent grade and were used as received without further purification. The ligand L (*N*,*N*′-bis[4-(4,5-dihydrooxazol-2-yl)-benzyl]ethane-1,2-diamine) was synthesized by procedures similar to those reported previously.[7] All procedures for synthesizing silver(I) complexes were carried out in the dark. The CHN microanalyses were carried out on a Perkin-Elmer 240C elemental analyzer at the Analysis Center of Nanjing University. FT-IR spectra were recorded in the range 400–4000 cm^{-1} on a Bruker Vector22 FT-IR spectrophotometer using KBr pellets. The luminescent spectra for the solid samples were recorded at room temperature on an Aminco Bowman Series 2 spectrophotometer with a xenon arc lamp as the light source, and all the measurements were carried out under the same conditions. Magnetic measurements in the temperature range 1.8–300 K were performed on a MPMS-SQUID magnetometer at a field of 2000 Oe on crystalline sample of **6** in the temperature-settle mode. The diamagnetic contributions were corrected by using Pascal's constants.

Syntheses

[AgL]CF_3SO_3 (1). A methanol solution (3 mL) of $AgCF_3SO_3$ (7.71 mg, 0.03 mmol) was added slowly to a solution of L (11.4 mg, 0.03 mmol) in methanol (3 mL) with stirring to give a clear solution. After several days, colorless needles were obtained by slow diffusion of diethyl ether into the reaction solution. Yield 43%. Anal. Calcd. for $C_{23}H_{26}AgF_3N_4O_5S$: C, 43.48; H, 4.12; N, 8.82; Found C, 43.42; H, 4.07; N, 8.81. IR(KBr, cm^{-1}): 1683(s), 1638(s), 1418(m), 1371(m), 1265(m), 1198(s), 1167(s), 1121(s), 1094(m), 941(m), 818(m), 797(w), 715(w), 677(w).

[AgL]CF_3SO_3 (2). A dichloromethane solution (2 mL) of L (11.4 mg, 0.03 mmol) was added slowly to a solution of $AgCF_3SO_3$ (7.71 mg, 0.03 mmol) in acetonitrile (1 mL) to give a clear solution. After several days, colorless crystals were obtained by slow diffusion of diethyl ether into the reaction solution. Yield 53%. Anal. Calcd. for $C_{23}H_{26}AgF_3N_4O_5S$: C, 43.48; H, 4.12; N, 8.82; Found C, 43.47; H, 4.13; N, 8.87. IR(KBr, cm^{-1}): 1635(s), 1572(w), 1518(w), 1420(m), 1376(s), 1341(m), 1266(s), 1158(s), 1097(s), 1054(s), 1031(s), 942(m), 819(m), 727(w), 678(w), 637(m), 572(w).

[Ag_2L_2]$(NO_3)_2$·$4CH_3NO_2$ (3). A buffer layer of methanol–nitromethane (1:1) solution (4 mL) was carefully layered over a solution of L (11.4 mg, 0.03 mmol) in nitromethane (3 mL). Then a solution of $AgNO_3$ (5.1 mg, 0.03 mmol) in methanol (3 mL) was layered over the buffer layer. Crystalline **3** was isolated after one week. Yield 13%. Anal. Calcd. for $C_{48}H_{64}Ag_2N_{14}O_{18}$: C,43.00; H,4.81; N, 14.62; Found C, 43.13; H, 4.72; N, 14.59. IR(KBr, cm^{-1}): 1636(s), 1572(w), 1513(w), 1368(s), 1259(s), 1096(m), 1018(m), 942(m), 841(w), 824(w), 743(w), 684(m).

[AgL]NO_3·$0.5CH_3OH$ (4). The title complex was prepared in a similar way to that for preparation of **1**, except that $AgNO_3$ was used instead of $AgCF_3SO_3$. Yield 21%. Anal. Calcd. For $C_{22.50}H_{28}AgN_5O_{5.50}$: C, 47.88; H, 5.00; N, 12.41; Found C, 47.73; H, 5.11; N, 12.49. IR(KBr, cm^{-1}): 1635(s), 1513(w), 1474(w), 1365(s), 1338(m), 1308(s), 1253(m), 1096(m), 1044(w), 1015(w), 943(m), 889(w), 850(w), 745(w), 684(m).

[AgL]BF_4 (5). Complex **5** was prepared in a similar way to that for preparation of **2**, except that $AgBF_4$ and methanol were used instead of $AgCF_3SO_3$ and dichloromethane, respectively. Yield 32%. Anal. Calcd. For $C_{22}H_{26}AgBF_4N_4O_2$: C, 46.10; H, 4.57; N,9.78; Found C, 46.15; H, 4.70; N, 9.71. IR(KBr, cm^{-1}): 1640(s), 1572(w), 1513(w), 1456(m), 1417(m), 1370(s), 1262(s), 1193(w), 1070(s), 942(m), 842(m), 742(w), 683(m), 521(w).

[$Cu_4L_2(OCH_3)_2(OH)_2(NO_3)_2$]$(NO_3)_2$·$0.32H_2O$ (6). A methanol solution (5 mL) of $Cu(NO_3)_2·6H_2O$ (7.2 mg, 0.03 mmol) was added to a solution of L (11.4 mg, 0.03 mmol) in methanol (5 mL) with stirring. The mixture was stirred for another 5 min and then left to stand at room temperature. Several days later, deep blue crystals were obtained. Yield 53%. Anal. Calcd. for $C_{46}H_{60.64}Cu_4N_{12}O_{20.32}$: C, 40.60; H, 4.49; N, 12.35; Found C 40.51, H 4.39, N 12.37. IR(KBr, cm^{-1}): 3423(m, br), 1715(w), 1641(s), 1573(w), 1515(w), 1367(s), 1261(s), 1108(s), 1076(m), 1044(m), 1019(m), 979(w), 944(m), 861(m), 796(w), 744(w), 697(m), 594(w).

X-Ray crystallography

The X-ray diffraction measurements for complexes **1–5** were performed on a Bruker Smart Apex CCD diffractometer with graphite-monochromated Mo-Kα radiation (λ = 0.71073 Å) at 293(2) K. Empirical absorption corrections were applied to the data by using the multiscan program SADABS.[8] Structures of **1–5** were solved by direct methods and refined by full-matrix least-square on F^2 using the SHELXTL program package.[9] All non-hydrogen atoms were refined anisotropically. The bond distances around N2 and disordered N1, the thermal factors of C1, C2 and disordered N1 in **1**, the C–N bond lengths in nitromethane in **3**, and the geometrical parameters and thermal factors of the disordered nitrate anions in **4** were restrained in the refinement. The hydrogen atoms of L ligands in **1–5** were generated geometrically, except those of C1, C2 and N1 in **1** were located directly. The N1 atom in complex **1** was disordered over two positions with site occupancy factors of 0.70 and 0.30, respectively. The diffraction data of **6** were collected on a Rigaku RAXIS-RAPID Imaging Plate diffractometer with graphite-monochromated Mo-Kα radiation (λ = 0.71075 Å) at 200 K. The structure of **6** was solved by direct methods using SIR92,[10] expanded using Fourier techniques DIRDIF94[11] and finally refined using SHELXL-97. The geometrical parameters and thermal factors of the disordered nitrate anions in **6** were restrained in the refinement. All the non-hydrogen atoms were refined anisotropically by the full-matrix least-squares method on F^2. The hydrogen atoms except those of the hydroxyl group and the free water molecule were generated geometrically. All calculations were performed using the teXsan crystallographic software package (Molecular Structure Corporation).[12] Details of the crystal parameters, data collection and refinements for

Table 1 Crystal data for complexes **1–6**

	1	**2**	**3**	**4**	**5**	**6**
Empirical formula	$C_{23}H_{26}AgF_3N_4O_5S$	$C_{23}H_{26}AgF_3N_4O_5S$	$C_{48}H_{64}Ag_2N_{14}O_{18}$	$C_{22.50}H_{28}AgN_5O_{5.50}$	$C_{22}H_{26}AgBF_4N_4O_2$	$C_{46}H_{60.64}Cu_4N_{12}O_{20.32}$
Formula weight	635.41	635.41	1340.87	564.37	573.15	1360.98
Crystal system	Monoclinic	Monoclinic	Triclinic	Monoclinic	Monoclinic	Monoclinic
Space group	$P2_1/c$	$P2_1/n$	$P\bar{1}$	$C2/c$	$C2/c$	$P2_1/c$
a (Å)	10.642(2)	17.0542(11)	5.5352(7)	14.0161(8)	15.250(9)	13.3839(19)
b (Å)	25.648(5)	7.8076(5)	11.4453(14)	8.7983(5)	8.2253(5)	15.715(2)
c (Å)	9.4569(19)	18.7729(12)	22.023(3)	40.648(2)	39.011(2)	26.095(4)
α (°)	90	90	82.720(2)	90	90	90
β (°)	97.89(3)	95.7930(10)	83.933(2)	98.3990(10)	100.4250(10)	94.420(5)
γ (°)	90	90	87.015(2)	90	90	90
V (Å^3)	2556.8(9)	2486.9(3)	1375.2(3)	4958.9(5)	4813(3)	5472.0(14)
Z	4	4	1	8	8	4
D_c (g cm^{-3})	1.651	1.697	1.619	1.512	1.582	1.663
μ (mm^{-1})	0.934	0.960	0.798	0.857	0.895	1.622
$F(000)$	1288	1288	688	2312	2320	2823
Reflns. collected	12614	14205	6872	12014	11524	39744
Independent reflns.	4509	5655	4769	4359	4240	9628
R_{int}	0.0225	0.0475	0.0207	0.0365	0.0243	0.0929
Parameters refined	343	322	364	331	330	775
Goodness-of-fit	1.025	1.053	0.984	1.226	1.137	1.102
R_1, wR_2[a] ($I > 2\sigma(I)$)	0.0697, 0.1867	0.0631, 0.1544	0.0777, 0.2188	0.0728, 0.1654	0.0614, 0.1578	0.0730, 0.1795
R_1, wR_2[a] (all data)	0.0852, 0.2026	0.0850, 0.1668	0.1015, 0.2367	0.0801, 0.1695	0.0703, 0.1638	0.0930, 0.1904

[a] $R_1 = \Sigma||F_o| - |F_c||/|F_o|$; $wR_2 = [\Sigma w(\Sigma F_o^2 - F_c^2)^2/\Sigma w(F_o^2)^2]^{1/2}$.

compounds **1–6** are summarized in Table 1. Selected bond lengths and angles for compounds **1–6** are listed in Table 2.

Results and discussion

Structure of [AgL]CF_3SO_3 (1)

The title complex crystallizes in monoclinic space group $P2_1/c$. There are one Ag(I) atom, one L ligand and one trifluoromethylsulfate anion in the repeat unit of **1**. As shown in Fig. 1a, each Ag(I) is four-coordinated, with distorted tetrahedral coordination geometry, by two nitrogen atoms of the ethylenediamine unit of one L ligand and two ones of the oxazoline group of two other L ligands. The N–Ag–N bond angles vary from 72.3(2)° to 134.9(3)° and the Ag–N bond distances are in the range from 2.248(5) to 2.459(5) Å (Table 2) with an average Ag–$N_{oxazoline}$ distance of 2.36 Å, which is longer than those in the reported Ag(I) complexes with oxazoline-containing ligands, for example [Ag(*S*,*S*-bbop)]CF_3SO_3 [bbop = 2,2-bis(4′-benzyloxazolin-2′-yl)propane] with an average Ag–$N_{oxazoline}$ bond length of 2.16 Å.[13] Therefore, three L ligands coordinate to one Ag(I) to achieve tetrahedral disposition of the four nitrogen atoms and in turn each L ligand connects three Ag(I) atoms. The L ligand in **1** has C-shape with a dihedral angle of 83.1° between the two terminal oxazolinyl planes. Such coordination mode makes complex **1** a wavelike 2D cationic network with (6,3) topology (Fig. 1b). A simplified 2D network where only the Ag(I) atoms are presented is shown in Fig. 1c. It can be seen that each six Ag(I) atoms form a hexagon with chair conformation (Fig. 1b and c), and the Ag···Ag distances are 8.75 Å for Ag1A···Ag1B, Ag1C···Ag1D, Ag1D···Ag1E and Ag1F···Ag1A and 7.95 Å for Ag1B···Ag1C and Ag1E···Ag1F (Fig. 1b), respectively. A similar woven structure has been observed in the complex [Ag(L1)]BF_4·CH_3CN,[14] in which the L1 ligand also adopted a C-shape, but in which the dihedral angle between the two terminal pyridyl rings is 6.7°. The vacancy formed between two adjacent 2D sheets is occupied by trifluoromethylsulfate anions, which are stabilized by two N–H···O [N2···O4^{i} 2.975(12) Å (symmetry code: i = x, y, 1 + z); N1–O3 3.235(17) Å] and two C–H···O [C19···O3^{ii} 3.273(16) Å (symmetry code: ii = x, $\frac{1}{2} - y$, $\frac{1}{2} + z$); C2···O5^{iii} 3.401(14) Å (symmetry code: iii = $1 - x$, $-y$, $1 - z$)] hydrogen bonds (Fig. 1d). The hydrogen bonding data are summarized in Table 3.

Structures of [AgL]CF_3SO_3 (2), [AgL]NO_3·0.5CH_3OH (4) and [AgL]BF_4 (5)

It is interesting to note that, when the same reaction of ligand L with $AgCF_3SO_3$ was carried out in dichloromethane and acetonitrile instead of methanol, a new complex **2** was obtained. The crystallographic analysis provides the direct evidence for the structure of **2**. Complexes **1** and **2** have the same composition and formula, but different structures, so they are supramolecular isomers.[15] The coordination environment around Ag(I) atom in **2** is the same as that in **1**, furthermore, each L ligand also links three Ag(I) atoms through its ethylenediamine moiety and two oxazoline groups as shown in Fig. 2a. However, the ligand L has a distorted C-shape in **2**, subtly different from that in **1**, resulting in the formation of the double-stranded helical chain (Fig. 2b), rather than the 2D network that appeared in **1**. The L ligand in **2** connects two Ag(I) atoms *via* the two oxazoline nitrogen atoms to produce a 1D helical chain with a pitch of 15.62 Å, which is further linked to another helical chain by the coordination bonds of ethylenediamine unit and Ag(I) to form a double-stranded helix with *P* and *M* forms (Fig. 2b). A similar Ag(I) complex containing the di-Schiff base ligand *N*,*N*′-bis(3-acetylpyridene)-idene-1,2-diaminoethane with a double-helix chain structure has been reported previously.[16] The 1D helices in **2** are stacked

Table 2 Selected bond distances (Å) and angles (°) for complexes **1–6**

1			
Ag(1)–N(4)	2.248(5)	Ag(1)–N(3)$^{\#2}$	2.358(6)
Ag(1)–N(1)$^{\#1}$	2.376(8)	Ag(1)–N(2)$^{\#1}$	2.459(5)
N(4)–Ag(1)–N(3)$^{\#2}$	115.6(2)	N(4)–Ag(1)–N(1)$^{\#1}$	134.9(3)
N(3)$^{\#2}$–Ag(1)–N(1)$^{\#1}$	102.5(3)	N(4)–Ag(1)–N(2)$^{\#1}$	114.7(2)
N(3)$^{\#2}$–Ag(1)–N(2)$^{\#1}$	107.62(18)	N(1)$^{\#1}$–Ag(1)–N(2)$^{\#1}$	72.3(2)
2			
Ag(1)–N(4)$^{\#3}$	2.306(4)	Ag(1)–N(3)$^{\#4}$	2.360(4)
Ag(1)–N(2)	2.390(4)	Ag(1)–N(1)	2.419(4)
N(4)$^{\#3}$–Ag(1)–N(3)$^{\#4}$	96.52(15)	N(4)$^{\#3}$–Ag(1)–N(2)	123.64(13)
N(3)$^{\#4}$–Ag(1)–N(2)	128.05(13)	N(4)$^{\#3}$–Ag(1)–N(1)	133.18(13)
N(3)$^{\#4}$–Ag(1)–N(1)	98.94(14)	N(2)–Ag(1)–N(1)	77.80(12)
3			
Ag(1)–N(4)$^{\#5}$	2.247(7)	Ag(1)–N(1)	2.278(7)
N(4)$^{\#5}$–Ag(1)–N(1)	170.6 (2)		
4			
Ag(1)–N(4)$^{\#6}$	2.311(5)	Ag(1)–N(3)$^{\#7}$	2.360(5)
Ag(1)–N(1)	2.390(5)	Ag(1)–N(2)	2.403(5)
N(4)$^{\#6}$–Ag(1)–N(3)$^{\#7}$	92.6(2)	N(4)$^{\#6}$–Ag(1)–N(1)	126.73(19)
N(3)$^{\#7}$–Ag(1)–N(1)	118.28(19)	N(4)$^{\#6}$–Ag(1)–N(2)	121.69(19)
N(3)$^{\#7}$–Ag(1)–N(2)	123.77(18)	N(1)–Ag(1)–N(2)	77.54(17)
5			
Ag(1)–N(1)$^{\#8}$	2.319(5)	Ag(1)–N(4)$^{\#9}$	2.362(5)
Ag(1)–N(3)	2.387(4)	Ag(1)–N(2)	2.431(4)
N(1)$^{\#8}$–Ag(1)–N(4)$^{\#9}$	91.70(17)	N(1)$^{\#8}$–Ag(1)–N(3)	126.61(16)
N(4)$^{\#9}$–Ag(1)–N(3)	121.16(17)	N(1)$^{\#8}$–Ag(1)–N(2)	119.58(15)
N(4)$^{\#9}$–Ag(1)–N(2)	125.13(16)	N(3)–Ag(1)–N(2)	76.79(14)
6			
Cu(1)–O(51)	1.943(5)	Cu(1)–O(52)	1.945(5)
Cu(1)–Cu(2)	2.9439(12)	Cu(2)–O(51)	1.944(5)
Cu(2)–O(52)	1.948(5)	Cu(3)–O(62)	1.939(5)
Cu(3)–O(61)	1.942(5)	Cu(3)–Cu(4)	2.8444(12)
Cu(4)–O(61)	1.937(5)	Cu(4)–O(62)	1.945(5)
O(51)–Cu(1)–O(52)	77.7(2)	O(51)–Cu(1)–O(11)	95.37(19)
O(11)–Cu(1)–Cu(2)	80.92(13)	O(52)–Cu(1)–O(11)	91.8(2)
O(51)–Cu(2)–O(52)	77.6(2)	O(52)–Cu(2)–O(12)	92.3(2)
O(51)–Cu(2)–O(12)	94.1(2)	O(62)–Cu(3)–O(61)	81.5(2)
O(62)–Cu(3)–O(21)	97.6(2)	O(61)–Cu(3)–O(21)	95.4(2)
O(61)–Cu(4)–O(22)	95.8(2)	O(61)–Cu(4)–O(62)	81.4(2)
O(62)–Cu(4)–O(22)	92.1(2)		

Symmetry transformations used to generate equivalent atoms: #1 x, $\frac{1}{2}-y$, $\frac{1}{2}+z$; #2 $-x$, $\frac{1}{2}+y$, $\frac{3}{2}-z$; #3 x, $y+1$, z; #4 x, $y-1$, z; #5 $-x+2$, $-y$, $-z$; #6 $x+\frac{1}{2}$, $y+\frac{1}{2}$, z; #7 $x-\frac{1}{2}$, $y-\frac{1}{2}$, z; #8 x, $y-1$, z; #9 x, $y+1$, z.

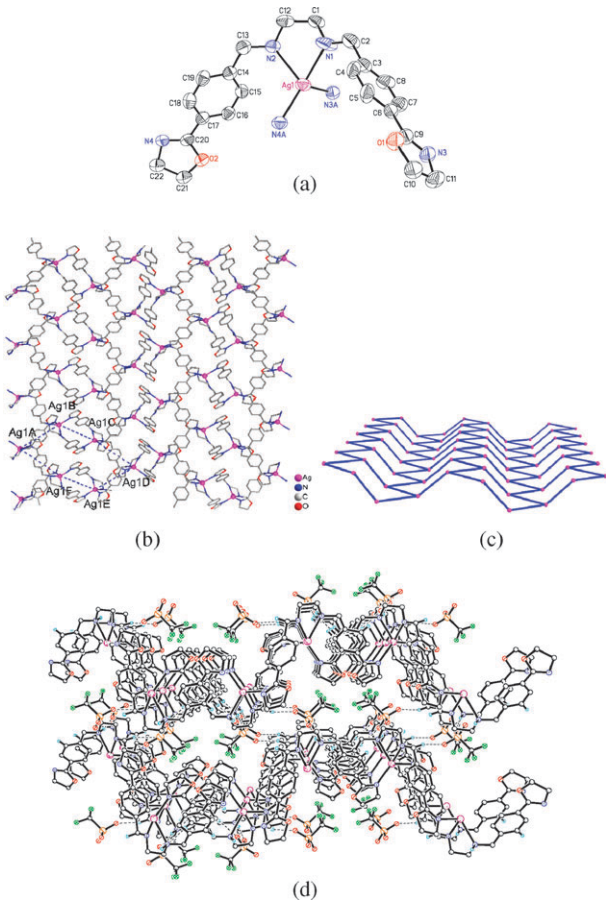

Fig. 1 (a) The coordination environment of Ag(I) in **1** with the ellipsoids drawn at the 30% probability level. The hydrogen atoms and trifluromethanesulfonate anion are omitted for clarity. Symmetry codes: N3A = $-x, -y+1, -z$; N4A = $x, -y+\frac{1}{2}, z-\frac{1}{2}$. (b) The 2D wavelike cationic network of **1**. (c) Schematic representation 2D network of **1** where only the silver(I) atoms are presented. (d) Crystal packing diagram of **1** with hydrogen bonds indicated by the dashed lines.

in a $\cdots PMPM\cdots$ repeating mode, hence the bulk crystals of **2** were obtained as a *meso*-compound. The trifluoromethylsulfate counteranions are fixed through two N–H···O [N1···O3 3.229(6) Å, N2···O3^{ii} 3.136(6) Å, symmetry code: ii = $x, -1+y, z$] hydrogen bonds to the double-stranded helices (Table 3).

Complexes **4** and **5** have the same double-stranded helical chain structure as **2**, and thus the structural descriptions of **4** and **5** are omitted here.

Structure of $[Ag_2L_2](NO_3)_2{\cdot}4CH_3NO_2$ (3)

In contrast to the polymeric structure of **1**, **2**, **4** and **5**, complex **3** is a dinuclear $[Ag_2L_2]^{2+}$ rectangle, which lies about an inversion centre, as shown in Fig. 3a. It is noticeable that each L with extended Z-shape acts as a bis-monodentate (rather than a tetradentate) ligand, using its two oxazoline nitrogen atoms to bind two Ag(I) atoms while the nitrogen atoms of ethylenediamine unit do not take part in coordination, as was observed in $[Co(L2)_2(SCN)_2]{\cdot}EtOH$.[6c] In turn, each Ag(I) atom links two L ligands with a N1–Ag1–N4A bond angle of 170.6(2)° to form a 38-membered M_2L_2 macrocyclic rectangle. The bond lengths of Ag1–N1 and Ag1–N4A are 2.274(6) and 2.237(5) Å and the intermetallic distance of Ag1···Ag1A is 18.2136(22) Å. The rectangles are further linked together *via* nitrate anions through Ag···O weak interactions [Ag1···O3 2.78 Å, Ag1···O5 2.66 Å, Ag1···O3^{iii} 2.81 Å, Ag1···O4^{iii} 2.80 Å, symmetry code: iii = $x, y+1, z$] (Fig. 3b) to generate a 1D tube with dimensions of 6.30 × 16.36 Å^2 along the *a* axis (Fig. 3c). The shortest intermetallic distance (Ag···Ag) between two adjacent rectangles is 5.54 Å. The nitromethane molecules are located in the interstices between the metallocyclic rectangles and are held there *via* two C–H···O (nitromethane) and three N–H···O hydrogen bonds (Table 3). The 1D tubes are further connected together through C–H···O (nitrate) hydrogen bonds to form a 2D network (Fig. 3d).

Table 3 Hydrogen bond distances (Å) and angles (°) for complexes **1–6** (D: donor; A: acceptor)

D–H···A	Distance D···A	D–H–A	Angle D–H–A
1			
N(2)–H(2A)···O(4)$^{\#1}$	2.981(12)	N(2)–H(2A)–O(4)$^{\#1}$	166
N(1)–H(1A)···O(3)	3.204(17)	N(1)–H(1A)–O(3)	139
C(19)–H(19)···O(3)$^{\#2}$	3.261(15)	C(19)–H(19)–O(3)$^{\#2}$	160
C(2)–H(2C)···O(5)$^{\#3}$	3.401(14)	C(2)–H(2C)–O(5)$^{\#3}$	173
2			
N(1)–H(1C)···O(3)	3.229(6)	N(1)–H(1C)–O(3)	147
N(2)–H(2C)···O(3)$^{\#4}$	3.136(6)	N(2)–H(2C)–O(3)$^{\#4}$	142
C(7)–H(7A)···O(5)$^{\#5}$	3.201(8)	C(7)–H(7A)–O(5)$^{\#5}$	124
3			
N(2)–H(2A)···O(6)$^{\#6}$	2.873(7)	N(2)–H(2A)–O(6)$^{\#6}$	153(6)
N(3)–H(3A)···O(8)	3.008(7)	N(3)–H(3A)–O(8)	111(5)
N(3)–H(3A)···O(9)	2.877 (8)	N(3)–H(3A)–O(9)	165(6)
C(11)–H(11A)···O(6)$^{\#7}$	3.177(8)	C(11)–H(11A)–O(6)$^{\#7}$	128
C(12)–H(12B)···O(9)$^{\#8}$	3.238(9)	C(12)–H(12B)–O(9)$^{\#8}$	132
C(21)–H(21B)···O(3)$^{\#7}$	3.250(11)	C(21)–H(21B)–O(3)$^{\#7}$	129
C(22)–H(22B)···O(4)$^{\#9}$	3.265(11)	C(22)–H(22B)–O(4)$^{\#9}$	131
C(22)–H(22B)···O(5)$^{\#10}$	3.035(11)	C(22)–H(22B)–O(5)$^{\#10}$	116
4			
C(2)–H(2C)···O(4)$^{\#11}$	3.267(14)	C(2)–H(2C)–O(4)$^{\#11}$	128
C(7)–H(7A)···O(7)$^{\#11}$	3.49(3)	C(7)–H(7A)–O(7)$^{\#11}$	174
C(15)–H(15A)···O(3)$^{\#11}$	3.358(7)	C(15)–H(15A)–O(3)$^{\#11}$	149
C(22)–H(22A)···O(1)$^{\#12}$	3.242(10)	C(22)–H(22A)–O(1)$^{\#12}$	130
C(22)–H(22B)···O(8)$^{\#13}$	3.50(3)	C(22)–H(22B)–O(8)$^{\#13}$	158
5			
C(7)–H(7A)···F(2)	3.344(10)	C(7)–H(7A)–F(2)	162
C(11)–H(11A)···F(1)$^{\#14}$	3.236(9)	C(11)–H(11A)–F(1)$^{\#14}$	129
6			
N1–H1···O21$^{\#15}$	3.229(8)	N1–H1–O21$^{\#15}$	142
N2–H2···O43	3.136(11)	N2–H2–O43	123
N3–H3···O71	3.241(6)	N3–H3–O71	147
N4–H4···O32	3.003(10)	N4–H4–O32	161
C3–H9···O42$^{\#16}$	3.171(11)	C3–H9–O42$^{\#16}$	121
C4–H11···O13$^{\#17}$	3.242(10)	C4–H11–O13$^{\#17}$	127
C10–H13···O23$^{\#15}$	3.156(10)	C10–H13–O23$^{\#15}$	133
C15–H17···O51	3.293(9)	C15–H17–O51	152
C16–H18···O61	3.355(9)	C16–H18–O61	146
C25–H23···O52	3.351(9)	C25–H23–O52	160
C26–H24···O62	3.306(9)	C26–H24–O62	147
C30–H26···O41	3.49(2)	C30–H26–O41	158
C35–H29···O52	3.310(9)	C35–H29–O52	156
C36–H30···O62	3.338(9)	C36–H30–O62	149
C40–H32···O13$^{\#17}$	3.374(8)	C40–H32–O13$^{\#17}$	145
C45–H35···O51	3.419(9)	C45–H35–O51	160
C46–H36···O61	3.249(9)	C46–H36–O61	148
C202–H47···O42$^{\#18}$	3.343(11)	C202–H47–O42$^{\#18}$	144
C202–H48···O31$^{\#19}$	3.304(12)	C202–H48–O31$^{\#19}$	142
C302–H51···O43$^{\#20}$	3.213(16)	C302–H51–O43$^{\#20}$	161
C302–H52···O13$^{\#21}$	3.175(12)	C302–H52–O13$^{\#21}$	138
C402–H55···O22$^{\#22}$	3.214(10)	C402–H55–O22$^{\#22}$	133
C402–H55···O23$^{\#22}$	3.204(10)	C402–H55–O23$^{\#22}$	161
C402–H56···O41$^{\#20}$	3.080(15)	C402–H56–O41$^{\#20}$	145

Symmetry transformations used to generate equivalent atoms: #1 $x, y, 1 + z$; #2 $x, \frac{1}{2} - y, \frac{1}{2} + z$; #3 $1 - x, -y, 1 - z$; #4 $\frac{3}{2} - x, \frac{1}{2} + y, \frac{3}{2} - z$; #5 $x, -1 + y, z$; #6 $2 - x, -y, -z$; #7 $1 - x, -y, -z$; #8 $1 + x, y, z$; #9 $-1 + x, y, 1 + z$; #10 $-2 + x, y, 1 + z$; #11 $-\frac{1}{2} + x, -\frac{1}{2} + y, z$; #12 $-\frac{1}{2} + x, -\frac{3}{2} + y, z$; #13 $-1 + x, -1 + y, z$; #14 $1 - x, 1 + y, \frac{1}{2} - z$; #15 $-x, 1 - y, 1 - z$; #16 $1 - x, 1 - y, 1 - z$; #17 $x, \frac{3}{2} - y, -\frac{1}{2} + z$; #18 $x, \frac{1}{2} - y, \frac{1}{2} + z$; #19 $-x, -\frac{1}{2} + y, \frac{3}{2} - z$; #20 $1 - x, \frac{1}{2} + y, \frac{3}{2} - z$; #21 $1 - x, 1 - y, 2 - z$; #22 $x, \frac{3}{2} - y, \frac{1}{2} + z$.

Structure of $[Cu_4L_2(OCH_3)_2(OH)_2(NO_3)_2](NO_3)_2{\cdot}0.32H_2O$ (6)

In contrast to the linear two- and tetrahedral four-coordinated Ag(I) in **1–5**, Cu(II) can have different coordination number and geometries. To investigate the effect of the metal ion on the structure of the complex, $Cu(NO_3)_2{\cdot}6H_2O$ was reacted with ligand L, and **6** was isolated. As shown in Fig. 4a, complex **6** consists of a cage-like dication unit $[Cu_4L_2(NO_3)_2(OCH_3)_2(OH)_2]^{2+}$ with two different kinds of Cu_2O_2 units linked by two U-shaped L ligands. In the Cu1O_2Cu2 subunit, each Cu(II) is five-coordinated with square-pyramid (τ = 0.02 for Cu1 and 0.01 for Cu2)[17] coordination geometry

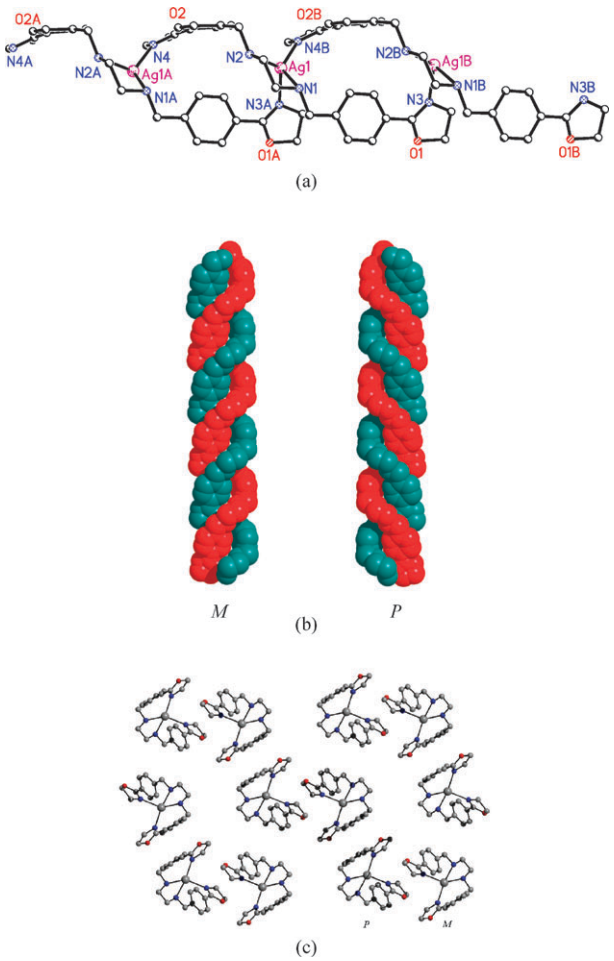

Fig. 2 (a) The crystal structure of **2**. The hydrogen atoms and trifluoromethanesulfate anions are omitted for clarity. Symmetry codes: A = x, $y - 1$, z; B = x, $y + 1$, z. (b) Space-filling diagram of double-stranded helical chains in **2** with *P* and *M* forms. (c) Crystal packing diagram of **2** showing the relationship of *P* and *M* forms.

by two oxygen (O51 and O52) atoms from the methoxoyl bridging groups, two nitrogen atoms from the oxazolinyl groups of L and one oxygen atom of the nitrate anion. The Cu–$O_{methoxo}$ bond lengths, which are in the range 1.943(5)–1.948(5) Å, as well as the Cu1···Cu2 and O51···O52 distances of 2.94 and 2.44 Å, are similar to those observed in the reported bis(μ-methoxo)dicopper(II) complexes.[18] In the case of $Cu3O_2Cu4$ subunit, the Cu(II) also exhibits a square-pyramidal coordination geometry (τ = 0.03 for Cu3 and 0.02 for Cu4), with the oxygen atom of the nitrate anion occupying the axial position. Two nitrogen atoms from the ethylenediamine unit of L ligand and two bridging hydroxyl oxygen (O61 and O62) atoms form the basal plane. The Cu–$O_{hydroxo}$ distances in the 1.937(5)–1.945(5) Å range are comparable to those reported for other μ^2-hydroxobridged dinuclear complexes.[19] The Cu3···Cu4 and O61···O62 distances are 2.84 and 2.53 Å, respectively. The averages of O–Cu–O angles for the methoxyl and hydroxyl bridges are 98.38 and 94.26°, respectively.

Of interest is the unusual bridging mode of L ligands. Two Cu_2O_2 subunits are linked together by two U-shaped L ligands

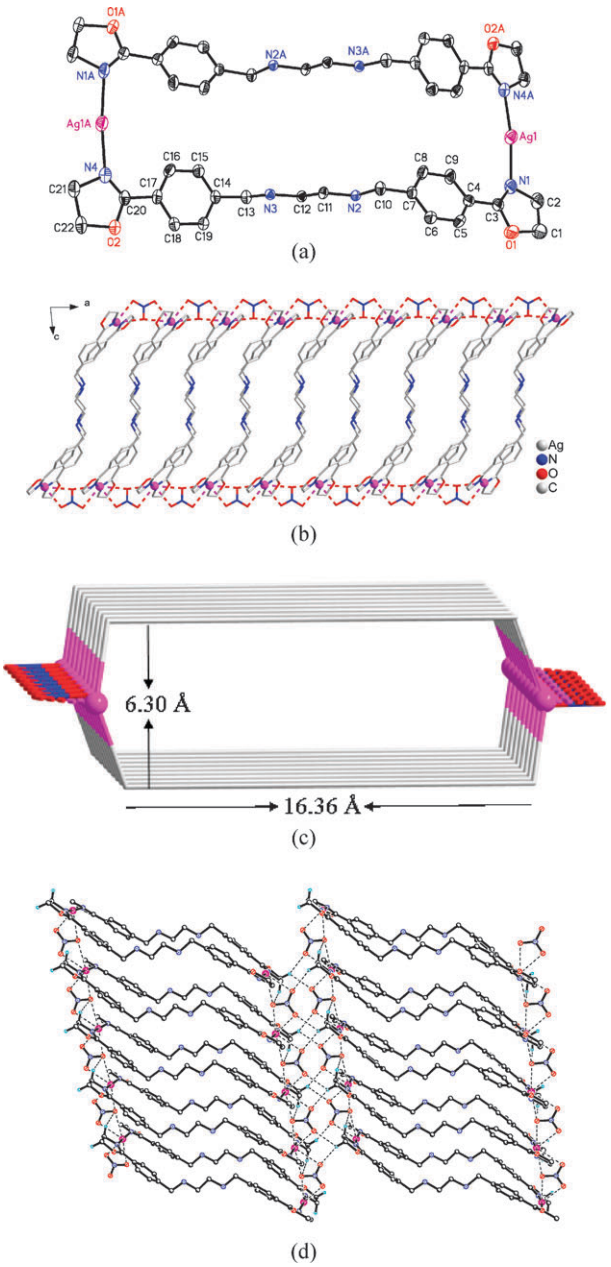

Fig. 3 (a) The crystal structure of **3**. The hydrogen atoms, nitrate anions and nitromethane molecules are omitted for clarity. Symmetry code: A = 2 − x, −y, −z. (b) 1D tubelike structure of **3**. (c) Schematic drawing of the tubelike structure of **3** in which the L ligands are simplified to straight lines linking the two coordinating nitrogen atoms. (d) 2D network of **3** with hydrogen bonds indicated by the dashed lines.

to give a cage-like tetranuclear structure, in which the Cu1···Cu3 and Cu2···Cu4 distances separated by L ligands are 7.05 and 7.01 Å, respectively. The M_4L_2 cationic cages are further linked together through N–H···O and C–H···O hydrogen bonds (Table 3) to produce a 3D structure (Fig. 4b).

Luminescence properties

The photoluminescence of ligand L and complexes **1–6** were studied in the solid state at room temperature. An emission at

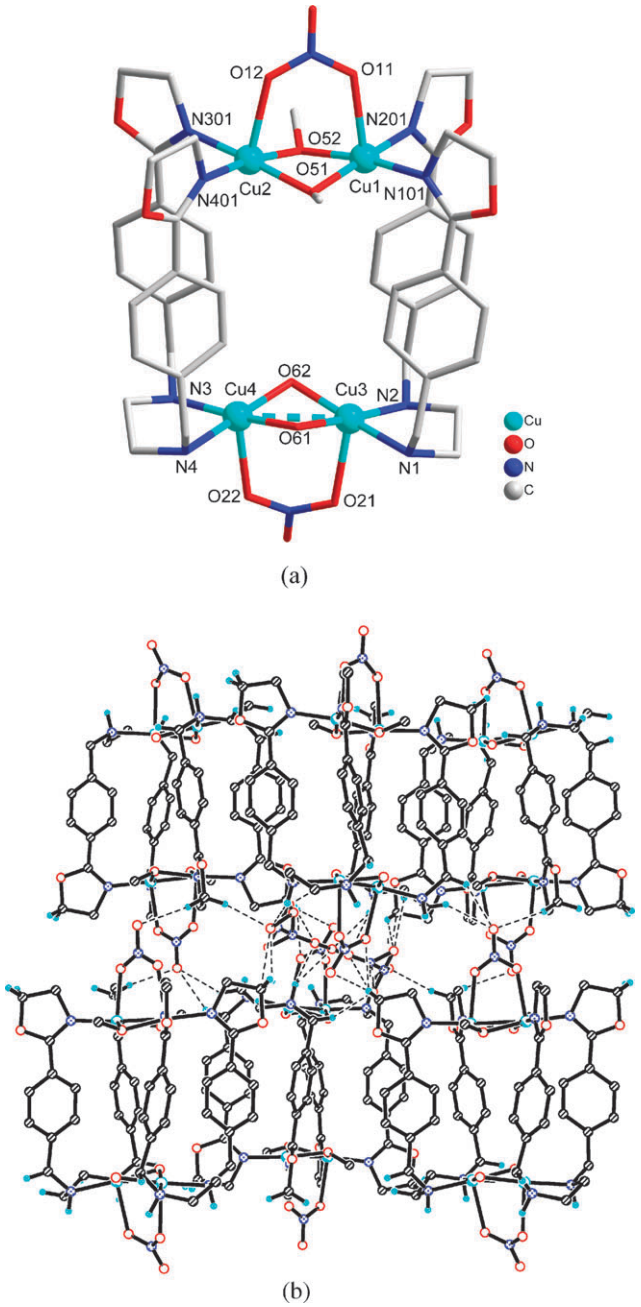

Fig. 4 (a) The structure of $[Cu_4L_2(CH_3O)(OH)(NO_3)_2]^{2+}$ in **6**. (b) Crystal packing diagram of **6** with hydrogen bonds indicated by the dashed lines.

429 nm was observed for complex **1** upon excitation at 364 nm, and the free ligand L displays luminescence with an emission maximum at 419 nm upon excitation at 357 nm, as illustrated in Fig. 5. Therefore, the observed luminescence of complex **1** can be tentatively assigned to the intraligand fluorescence emission due to their similarity.[20] The observed red-shift (10 nm) of emission for complex **1** compared with that for the free ligand L, accompanied by an increase of luminescence intensity, may be attributed to the coordination of the L ligand to the silver ions.[21] However, no clear photoluminescence was observed for the complexes **2–6** under the experimental conditions used. Complexes **2–5** have different structures to **1**,

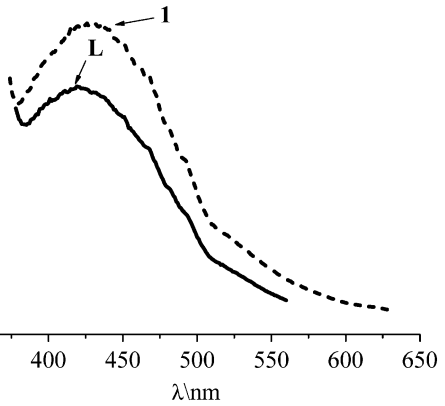

Fig. 5 The emission spectra of ligand **L** (solid line) with λ_{exc} = 357 nm and complex **1** (dotted line) with λ_{exc} = 364 nm in the solid state at room tempetature.

and the silver(I) complexes have been reported to show weak or no luminescence at room temperature,[22] while for complex **6** the luminescence may be quenched by the Cu(II) ion. The results imply that the luminescence is greatly influenced by central metal ion and the structure of the complexes.

Magnetic properties

The crystal structure of complex **6** showed that there are $Cu_2(OCH_3)_2$ and $Cu_2(OH)_2$ dimeric units (Fig. 4a), and thus magnetic interactions may be expected between the Cu(II) atoms bridged by methoxyl and hydroxyl groups. The distance of *ca.* 7.0 Å between the two Cu_2O_2 units is long, so that the magnetic interactions between the two Cu_2O_2 units can be neglected. Magnetic measurements were performed on crystalline sample of **6** at an applied magnetic filed of 2000 Oe in the temperature range 1.8–300 K, and the plots of χ_M *vs.* T and $\chi_M T$ *vs.* T are shown in Fig. 6a. The $\chi_M T$ is 1.35 emu K mol^{-1} at 300 K, which is smaller than the spin-only value of 1.5 emu K mol^{-1} (g = 2) and decreases gradually upon cooling to 1.07 emu K mol^{-1} at 80 K. For the O-bridged copper(II) complexes, the magnetic properties are usually dictated by the Cu–O–Cu bridging angle. It has been reported that in the methoxyl-bridged Cu_2O_2 unit there is an antiferromagnetic interaction when the Cu–O–Cu angle is larger than 95.7° and a ferromagnetic interaction when the Cu–O–Cu angle is smaller than 95.7°.[19,23,24] In complex **6**, the methoxyl-bridged Cu1–O51–Cu2 and Cu1–O52–Cu2 angles are 98.5(2) and 98.3(2)°, respectively, suggesting the presence of an antiferromagnetic intra-dimer interaction. The plot of χ_M^{-1} *vs.* T is shown in Fig. 6b, which exhibits a linear relation above 115 K. The temperature dependence of magnetic susceptibilities above 115 K obeys the Curie–Weiss law $\chi_M = C/(T - \theta)$ with Weiss constant $\theta = -40$ K, and Curie constant C = 1.38 emu K mol^{-1}. The negative value of θ shows the antiferromagnetic interaction. Between 80 K and 8 K, the $\chi_M T$ is fairly constant, indicating almost no magnetic interactions between the two copper ions Cu3 and Cu4. At very low temperature (below 8 K), the $\chi_M T$ decreases rapidly, indicating very weak antiferromagnetic interactions, may come from intermolecular interactions between copper units

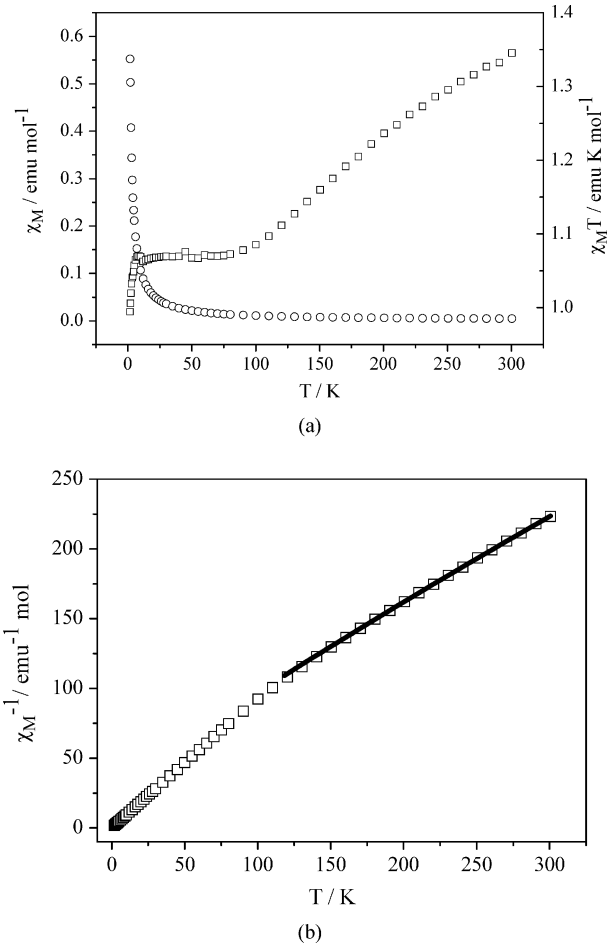

Fig. 6 (a) Temperature dependence of the $\chi_M T$ (□) and χ_M (○) for complex **6**. (b) Temperature dependence of $\chi_M{}^{-1}$ for complex **6**. The solid lines represent the best fit of the lines.

(through short contacts), and/or could be mediated by the nitrate bridging units.[25]

Conclusion

The present study shows that the reaction of a new flexible multidentate ligand L with various metal salts can afford a variety of MOFs, in which the flexible ligand L can have different conformation to fit the geometrical requirement of metal ions. In complex **1**, ligand L adopts a C-shape to gave a (6,3) topological 2D network, while the distorted C-shape of L ligand in **2**, **4** and **5** results in the formation of a double-helical chain. In the case of complexes **3** and **6**, the ligands L have extended Z- and U-shapes, leading to the formation of a M_2L_2 macrocyclic rectangle (**3**) and a M_4L_2 cage (**6**), respectively. The results show that the new oxazoline-containing tetradentate ligand L is versatile for the construction of new MOFs.

Acknowledgements

This work was financially supported by the National Natural Science Foundation of China (Grant no. 20828002, 20731004 and 20721002) and the National Basic Research Program of China (Grant no. 2007CB925103 and 2010CB923303).

References

1 (*a*) T. T. Luo, H. C. Wu, Y. C. Jao, S. M. Huang, T. W. Tseng, Y. S. Wen, G. H. Lee, S. M. Peng and K. L. Lu, *Angew. Chem., Int. Ed.*, 2009, **48**, 9461; (*b*) G. Férey, *Chem. Soc. Rev.*, 2008, **37**, 191; (*c*) R. A. Fisher and C. Wöll, *Angew. Chem., Int. Ed.*, 2008, **47**, 8164; (*d*) S. Ma, D. Yuan, X. S. Wang and H. C. Zhou, *Inorg. Chem.*, 2009, **48**, 2072; (*e*) P. K. Thallapally, J. Tian, M. R. Kishan, C. A. Fernandez, S. J. Dalgarno, P. B. McGrail, J. E. Warren and J. L. Atwood, *J. Am. Chem. Soc.*, 2008, **130**, 16842.
2 (*a*) L. Hou, Y. Y. Lin and X. M. Chen, *Inorg. Chem.*, 2008, **47**, 1346; (*b*) B. T. N. Pham, L. M. Lund and D. Song, *Inorg. Chem.*, 2008, **47**, 6329; (*c*) H. J. Liu, X. T. Tao, Y. X. Yan, Y. Ren, H. P. Zhao, Q. Xin, W. T. Yu and M. H. Jiang, *Cryst. Growth Des.*, 2008, **8**, 259; (*d*) A. Lan, K. Li, H. Wu, D. H. Olson, T. J. Emge, W. Ki, M. Hong and J. Li, *Angew. Chem., Int. Ed.*, 2009, **48**, 2334.
3 (*a*) E. Coronado, J. R. Galán-Mascarós and C. Martí-Gastaldo, *J. Am. Chem. Soc.*, 2008, **130**, 14987; (*b*) X. N. Cheng, W. Xue, J. B. Lin and X. M. Chen, *Chem. Commun.*, 2010, **46**, 246; (*c*) H. P. Jia, W. Li, Z. F. Ju and J. Zhan, *Chem. Commun.*, 2008, 371; (*d*) K. L. Hu, M. Kuromo, Z. Wang and S. Gao, *Chem. Eur. J.*, 2009, **15**, 12050.
4 (*a*) M. Tonigold, Y. Lu, B. Bredenkötter, B. Rieger, S. Bahnmüller, J. Hitzbleck, G. Langstein and D. Volkmer, *Angew. Chem., Int. Ed.*, 2009, **48**, 7546; (*b*) B. Kesanli and W. B. Lin, *Coord. Chem. Rev.*, 2003, **246**, 305; (*c*) K. K. Tanabe and S. M. Cohen, *Angew. Chem., Int. Ed.*, 2009, **48**, 7424; (*d*) J. S. Seo, D. Whang, H. Lee, S. I. Jun, J. Oh, Y. J. Jeon and K. Kim, *Nature*, 2000, **404**, 982; (*e*) Z. Wang, G. Chen and K. Ding, *Chem. Rev.*, 2009, **109**, 322; (*f*) S. Hasegawa, S. Horike, R. Matsuda, S. Furukawa, K. Mochizuki, Y. Kinoshita and S. Kitagawa, *J. Am. Chem. Soc.*, 2007, **129**, 2607.
5 (*a*) A. Harada, *Acc. Chem. Res.*, 2001, **34**, 456; (*b*) C. Marchal, Y. Filinchuk, X. Y. Chen, D. Imbert and M. Mazzanti, *Chem. Eur. J.*, 2009, **15**, 5273; (*c*) A. K. Bar, R. Chakrabarty and S. Munherjee, *Inorg. Chem.*, 2009, **48**, 10880; (*d*) J. Wang, Z. J. Lin, Y. C. Ou, Y. Shen, R. Herchel and M. L. Tong, *Chem. Eur. J.*, 2008, **14**, 7218.
6 (*a*) B. L. Fei, W. Y. Sun, K. B. Yu and W. X. Tang, *J. Chem. Soc., Dalton Trans.*, 2000, 805; (*b*) W. Y. Sun, B. L. Fei, T. a. Okamura, W. X. Tang and N. Neyama, *Eur. J. Inorg. Chem.*, 2001, 1855; (*c*) X. M. Ouyang, B. L. Fei, T. a. Okamura, H. W. Bu, W. Y. Sun, W. X. Tang and N. Ueyama, *Eur. J. Inorg. Chem.*, 2003, 618.
7 (*a*) M. Felderhoff, T. Smolka, R. Sustmann, I. Steller, H.-C. Weiss and R. Boese, *J. Prakt. Chem.*, 1999, **341**, 639; (*b*) H. Witte and W. Seeliger, *Angew. Chem., Int. Ed. Engl.*, 1972, **11**, 287.
8 G. M. Sheldrick, *SADABS, Program for Bruker Area Detector Absorption Correction*, University of Göttingen, Göttingen, Germany, 1997.
9 *SHELXTL*, version 6.12 Bruker Analytical Instrumentation, Madison, WI, 2000.
10 *SIR92*: A. Altomare, M. C. Brula, M. Camalli, M. Cascarano, C. Giacovazzo, A. Guagliardi and G. Polidori, *J. Appl. Cryst.*, 1994, **27**, 435.
11 *DIRDIF94*: P. T. Beurskens, G. Admiraal, G. Beurskens, W. P. Bosman, R. De Gelder, R. Israel and J. M. M. Smits, *The DIRDIF-94 program system*, Technical Report of the Crystallography Laboratory, University of Nijmegen, The Netherlands, 1994.
12 *teXsan*: Crystal Structure Analysis Package, Molecular Structure Corporation, 1985 and 2004.
13 S. M Ma and S. L. Wu, *New J. Chem.*, 2001, **25**, 1337.
14 B. L. Fei, W. Y. Sun, Y. A. Zhang, K. B. Yu and W. X. Tang, *Inorg. Chim. Acta*, 2000, **306**, 106.
15 (*a*) M. F. Wu, F. K. Zheng, G. Xu, A. Q. Wu, Y. Li, H. F. Chen, S. P. Guo, F. Chen, Z. F. Liu, G. C. Guo and J. S. Huang, *Inorg. Chem. Commun.*, 2010, **13**, 250; (*b*) R. W. Seidel, R. Goddard, K. Focker and I. M. Oppel, *CrystEngComm*, 2010, **12**, 387; (*c*) W. G. Lu, K. Yang, L. Jiang, X. L. Feng and T. B. Lu, *Inorg. Chim. Acta*, 2009, **362**, 5259; (*d*) X. C. Huang, D. Li and X. M. Chen, *CrystEngComm*, 2006, **8**, 351.
16 M. Sarkar and K. Biradha, *CrystEngComm*, 2004, **6**, 310.
17 A. W. Addison and T. N. Rao, *J. Chem. Soc., Dalton Trans.*, 1984, 1349.

18 M. Yamashita, H. Ito and T. Ito, *Inorg. Chem.*, 1983, **22**, 2101.
19 G. D. Munno, M. Julve, F. Lloret, J. Faus, M. Verdaguer and A. Caneschi, *Inorg. Chem.*, 1995, **34**, 157.
20 (*a*) Y. Wang, B. Ding, P. Cheng, D.-Z. Liao and S.-P. Yan, *Inorg. Chem.*, 2007, **46**, 2002; (*b*) B. Ding, L. Yi, Y. Wang, P. Cheng, D.-Z. Liao, S.-P. Yan, Z.-H. Jiang, H.-B. Song and H.-G. Wang, *Dalton Trans.*, 2006, 665.
21 (*a*) X. L. Wang, C. Qin, E. B. Wang and Z. M. Su, *Chem. Eur. J.*, 2006, **12**, 2680; (*b*) S. L. Zheng and X. M. Chen, *Aust. J. Chem.*, 2004, **57**, 703; (*c*) M. H. Shu, C. L. Tu, W. D. Xu, H. B. Jin and J. Sun, *Cryst. Growth Des.*, 2006, **6**, 1890.
22 M.-L. Tong, X.-M. Chen, B.-L. Ye and L.-N. Ji, *Angew. Chem., Int. Ed.*, 1999, **38**, 2237.
23 R. D. Willett and G. L. Breneman, *Inorg. Chem.*, 1983, **22**, 326.
24 P. Seppälä, E. Colacio, A. J. Mota and R. Sillanpää, *Inorg. Chim. Acta*, 2010, **363**, 755.
25 H. M. J. Hendriks, P. J. M. W. L. Birker, J. van Rijn, G. C. Verschoor and J. Reedijk, *J. Am. Chem. Soc.*, 1982, **104**, 3607.

